

# Uncertainty Bounds of Transmission Line Parameters Estimated from Synchronized Measurements

Markos Asprou, *Member, IEEE*, Elias Kyriakides, *Senior Member, IEEE*, and Mihaela Albu, *Senior Member, IEEE*

**Abstract**—The parameters of the transmission lines are used in several monitoring and control tools of the power system control center. An accurate knowledge of the power system model (including transmission lines impedances) impacts positively the situational awareness of the power system operators. It also improves the protection and corrective measures that may be applied in case of a disturbance. Nevertheless, line parameters that are stored in the control center database are typically subjected to errors and therefore it is necessary to regularly refine them. The presence of a Phasor Measurement Unit (PMU) at both ends of the transmission line allows the calculation of the transmission line parameters using synchronized current and voltage phasor measurements. Although the use of PMU measurements is a straightforward way to calculate the transmission line parameters, the uncertainty of the synchronized phasor measurements should be incorporated to the calculated transmission line parameter values. In this paper, an analytical expression for the bounds of the calculated transmission line parameters from PMU measurements is derived, considering both instrument transformers and PMU errors. The calculated bounds of uncertainty are evaluated through Monte Carlo simulations while the importance of knowing the bounds of the calculated line parameters is underlined through the derivation of Power-Voltage (P-V) curves considering the lower and upper bounds of the parameters. Simulation results are obtained using the IEEE 14-bus system.

**Index Terms**—Instrument transformers, measurement uncertainty, network model, phasor measurement unit, transmission line parameters

## I. INTRODUCTION

THE software tools in modern power system control centers rely heavily on the a priori knowledge of topology and network parameters. Unlike the topology of the system that might change throughout the day, the transmission line parameters are considered time invariant and they are stored in the control center databases. The stored values of the transmission line parameters are usually derived from manufacturers' data and typical line configurations. Although

in an ideal environment such a procedure would derive impedance values very close to the actual ones, this is not the case in the real field. Environmental factors (i.e., temperature and soil resistivity) [1], modelling inaccuracies such as those used for parallel transmission lines and joints of overhead transmission lines that may be connected to underground cables, and human factors (unreported changes in the network connectivity or line length miscalculation) cause the deviation of the stored line parameters values from the actual ones [2]. Some surveys have shown that the error between the stored line parameters (and consequently of the impedances) and the actual ones could be up to 30% [3]. Such errors could impact negatively the monitoring tools performance (such as the state estimator), resulting to misleading information for the power system operators [4].

Several methodologies were proposed in the literature to identify and estimate the erroneous transmission line parameters stored in the control center [5], [6], [7]. The majority of the methodologies are based on the estimated states of the system provided by the state estimator, while high measurement redundancy is required to successfully estimate all the erroneous transmission line parameters [8]. With the advent of Synchronized Measurement Technology, and the installation of PMUs in the measurement layer of power systems, information about the transmission line parameters can be updated through computations of simultaneously acquired measurements of voltages and currents. One could argue that the use of waveform samples (time-tagged) could be an alternative solution to the PMU measurements. However, due to the geographically-dependent frequency deviation in modern electricity grids with high share of RES-based generation, there is an imperative need for synchronously measured voltage and current phasors. In such case, a PMU is required at either end of the transmission line. Although, the presence of a PMU at either end of all the transmission lines in a power system is unusual today, electric utilities could identify suspicious transmission lines with erroneous parameters and install periodically mobile PMUs for calculating their parameters [9].

Manuscript received February 15, 2018; revised May 23 and July 6, 2018; accepted August 6, 2018. This project has received funding from the European Union's Horizon 2020 research and innovation programme under grant agreement No 774407.

M. Asprou and E. Kyriakides are with the KIOS Research and Innovation Center of Excellence and the Department of Electrical and Computer

Engineering, University of Cyprus, Nicosia, Cyprus (e-mail: asprou.markos@ucy.ac.cy, elias@ucy.ac.cy).

M. Albu is with the Department of Electrical Engineering, Politehnica University of Bucharest, Bucharest, Romania (e-mail: albu@ieee.org).

The calculation of the line parameters through PMU measurements is trivial and straightforward [10]; however, it is important to consider the uncertainties of the measured quantities in the calculation process [11]. According to [12], the knowledge about the uncertainties of the measured quantities can be utilized for calculating the bounds of the calculated parameters. Such information can be used in contingency analysis for assessing the power system operating conditions in case that actual line parameter values are close to the bounds [13]. Furthermore, the line parameter bounds can be used as settings in protection devices (i.e., impedance relays) or current differential protection schemes [14].

Some works have dealt with the uncertainties associated with the calculated parameters through PMU measurements. In [14], the range of the transmission line parameter variation is estimated through a multivariable optimization problem, considering only the uncertainties that are introduced to the measured synchrophasors by the PMU. In [15], the authors proposed a two-stage optimization problem to reduce the deviations in the calculated line parameters (from their nominal values) caused by the systematic errors that are introduced to the PMU measurements by the instrument transformers.

The estimation of the line parameters is also gaining attention in the distribution grid. In [16], the data from  $\mu$ PMUs were used for estimating the parameters of the distribution lines and the transformers and for identifying any inconsistencies between the model and the calculated parameters. The modeling uncertainties in the state estimation of the distribution grids including the uncertainties of the line parameters are considered in [17]. In [18], both systematic and random errors are considered for the estimation of the line parameters in the distribution grid, including the uncertainties of the instrument transformers and PMUs.

In this paper, analytical expressions of the uncertainties associated with the calculated line parameters through PMU measurements are derived. The expressions are derived by taking into consideration the maximum measurement errors of both the instrument transformers and the PMU. The consideration of the instrument transformers errors and especially the ones of the current transformers is very important for the calculation of an uncertainty close to the actual one. In particular, as it was shown in [19], the error of the line parameters calculated through PMU measurements varies according to the loading conditions of the system. This is due to the variation of the maximum error of the current transformers depending on the current that passes through them. Therefore, both voltage and current transformers' errors as well as PMU errors are considered in this paper, in order to derive the analytical expression of the uncertainties associated with the calculated line parameters. The bounds derived by the calculated uncertainties are validated through Monte-Carlo simulations, while they are used to extract P-V curves for the IEEE 14-bus system.

The rest of the paper is organized as follows: Section II describes briefly the way of calculating transmission line parameters through PMU measurements, while the measurement uncertainties associated with the PMU

measurements and the way of calculating the uncertainties of the line parameters are described in Section III. Simulation results for validating the calculated line parameter uncertainties and the usefulness of knowing the line parameter bounds are shown in Section IV, while Section V concludes the paper.

## II. CALCULATION OF LINE PARAMETERS THROUGH PMU MEASUREMENTS

Transmission lines are represented as an equivalent pi model in most of the monitoring tools of the power system control center (i.e., state estimator, power flow analysis, transient stability analysis). The corresponding model that is shown in Fig. 1, is described by four parameters, namely the series conductance ( $g_{sr}$ ), the series susceptance ( $b_{sr}$ ), the shunt conductance ( $g_{sh}$ ), and the shunt susceptance ( $b_{sh}$ ). It should be noted that the shunt conductance is negligible and it is usually omitted from the pi model. Given that synchronized current and voltage phasors are available from the two ends of the line through PMUs, the series admittance  $y_{sr}$  (including both the series conductance and susceptance) and the shunt admittance  $y_{sh}$  are calculated as,

$$y_{sh} = \frac{\tilde{I}_s - \tilde{I}_r}{\tilde{V}_s + \tilde{V}_r} \quad (1)$$

$$y_{sh} = \frac{\tilde{I}_s - \tilde{I}_r}{\tilde{V}_s + \tilde{V}_r} \quad (2)$$

where  $\tilde{V}_s$  and  $\tilde{V}_r$  are the voltage phasors of buses  $s$  and  $r$  respectively while  $\tilde{I}_s$  is the current phasor that flows from bus  $s$  and  $\tilde{I}_r$  is the current phasor that arrives to bus  $r$  as shown in Fig. 1.

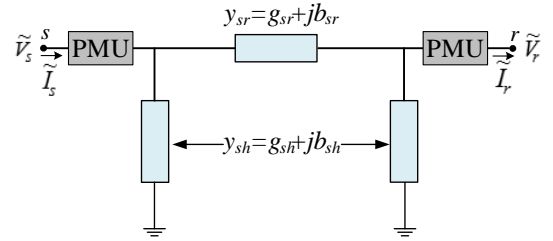


Fig. 1. Transmission line representation as a pi-model

By expressing the voltage and current phasors in rectangular form and substituting them in (1) and (2), the line parameters are expressed as a function of the voltage magnitude ( $V$ ), the voltage angle ( $\phi$ ), the current magnitude ( $I$ ), and the current angle ( $\theta$ ),

$$g_{sr} = \frac{A[V_s^2 \cos(c) - V_r^2 \cos(d)] + B[V_s^2 \cos(h) - V_r^2 \cos(l)]}{V_s^4 + V_r^4 - 2V_s^2 V_r^2 \cos(2\phi_s - 2\phi_r)} \quad (3)$$

$$b_{sr} = \frac{A[V_s^2 \sin(c) + V_r^2 \sin(d)] + B[V_s^2 \sin(h) + V_r^2 \sin(l)]}{V_s^4 + V_r^4 - 2V_s^2 V_r^2 \cos(2\phi_s - 2\phi_r)} \quad (4)$$

$$b_{sh} = \frac{I_s V_s \sin(\theta_s - \phi_s) - B \sin(h) - A \sin(d) + V_r I_r \sin(\phi_r - \theta_r)}{V_s^2 + V_r^2 + 2V_s V_r \cos(\phi_s - \phi_r)} \quad (5)$$

where,

$$A = I_s V_r \quad (6)$$

$$B = I_r V_s \quad (7)$$

$$c = \theta_s + \phi_r - 2\phi_s \quad (8)$$

$$d = \phi_r - \theta_s \quad (9)$$

$$h = \theta_r - \phi_s \quad (10)$$

$$l = 2\phi_r - \theta_r - \phi_s \quad (11)$$

The subscripts  $s$  and  $r$  in the above equations stand for the sending and receiving bus respectively of the transmission line. All the quantities that are used for calculating the transmission line parameters can be obtained through PMUs and consequently are subjected to measurement uncertainties.

### III. MEASUREMENT UNCERTAINTIES OF A PMU MEASUREMENT CHAIN AND CALCULATION OF LINE PARAMETER UNCERTAINTIES

The uncertainties associated with a measurement are introduced by the equipment used for obtaining the measurement, when the phenomena are following the abstract model used by the measurement system. In this work the model uncertainties are ignored, considering only the instrument uncertainties. In order to verify this assumption, the line parameters of the IEEE 14-bus system are represented with two different line models, namely the pi-model and the distributed line model. The voltage magnitude and voltage angle of the buses (extracted from the simulation) for the two models of the line are compared in order to realize the modelling error. The maximum bus voltage magnitude deviation (bus 5) is  $1.36 \times 10^{-4}$  p.u., while the maximum voltage angle deviation (bus 3) is 0.037 degrees. The average voltage magnitude deviation (considering all the buses) is  $5.9 \times 10^{-5}$  p.u., while the average angle deviation is 0.023 degrees. This confirms that for the purposes of the work presented in this paper, the modelling uncertainties can be ignored.

As it is shown in Fig. 2, in the case of the PMU measurements, two main components exist in the measurement chain, namely the instrument transformers and the PMU. The instrument transformers are used for stepping down the level of the grid voltage and current to an acceptable level before entering the PMU. Thus, in most of the PMU measurement chains with PMUs that require instrument transformer inputs (except the ones that PMUs are connected to merging units) there is always a voltage and a current transformer that are connected to the PMU through cables.

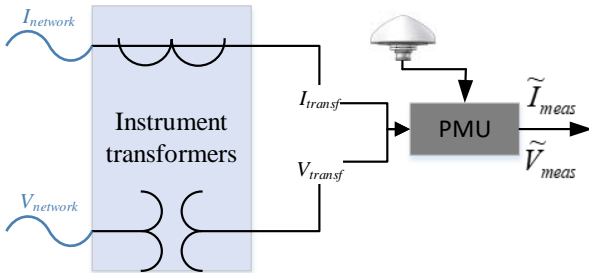


Fig. 2. PMU measurement chain

Both components of the PMU measurement chain introduce an uncertainty to the obtained measurement which can be evaluated through two ways: The Type A and the Type B evaluation method [12]. In the Type A evaluation method, the uncertainty is approximated from the repeated observations of the measurement process under the same operational and environmental conditions. However, the Type A evaluation method cannot be applied to the power system field since the operating conditions change continuously.

In the Type B evaluation method, the measurement uncertainty is approximated through the information provided by the manufacturers of the measurement chain components. In particular, for the accurate calculation of the standard uncertainty associated with the measurement chain in Fig. 2, the measurement errors are treated as random variables whose distribution for each component (i.e., instrument transformers and PMU) should be known. This is because the measurement uncertainty is the variance of the error distribution. According to the GUM, the uncertainties of a calculated quantity can be used for specifying the bounds of the respective quantity. More specifically, in order to include a large portion of the distribution of values that could be attributed to the calculated quantity, the expanded uncertainty can be used to define an interval that the calculated quantity lies. In order to calculate the expanded uncertainty a coverage factor  $k$  that usually takes values from 2 to 3 is used.

However, the manufacturer data sheets of both the instrument transformer and the PMU, report only the error bounds without any explicit information about the distribution of the error. In such case, a uniform error distribution should be assumed according to the GUM (Guide to the expression of Uncertainty in Measurements). In this sense, the PMU measurements can be expressed as,

$$V_{meas} \approx V_{network} (1 + \text{unif}(\bar{e}_{VT}^V) + \text{unif}(\bar{e}_{PMU}^V)) \quad (12)$$

$$I_{meas} \approx I_{network} (1 + \text{unif}(\bar{e}_{CT}^I) + \text{unif}(\bar{e}_{PMU}^I)) \quad (13)$$

$$\phi_{meas} = \phi_{network} + \text{unif}(\bar{e}_{VT}^\phi) + \text{unif}(\bar{e}_{PMU}^\phi) \quad (14)$$

$$\theta_{meas} = \theta_{network} + \text{unif}(\bar{e}_{VT}^\theta) + \text{unif}(\bar{e}_{PMU}^\theta), \quad (15)$$

where,

$\text{unif}(\bullet)$  denotes the symmetric uniform distribution with zero mean value whose limits are specified in the parenthesis. In the expressions (12)-(15) a random sample from the uniform distribution is used for adding random errors in the PMU measurements.

$\bar{e}_{VT}^V, \bar{e}_{CT}^I, \bar{e}_{PMU}^V, \bar{e}_{PMU}^I$ , are the voltage and current magnitude maximum errors, while  $\bar{e}_{VT}^\phi, \bar{e}_{CT}^\theta, \bar{e}_{PMU}^\phi, \bar{e}_{PMU}^\theta$ , are the voltage and current angle maximum errors. It should be noted that the maximum voltage and current magnitude errors are expressed as a percentage. Therefore, in (12) and (13) the voltage and current magnitudes of the network ( $V/I_{network}$ ), which are the error free quantities (Fig. 2), enter in the measurement chain and therefore they are multiplied by a random sample from the two uniform distributions (PMU and ITs). Furthermore, the measured voltage and current magnitudes are approximately equal to the expressions in (12) and (13). This because the product of the uniform distributions that should exist in (12) and (13) would result in a very small number that could be neglected. According to [20], this assumption is valid since the

multiplication of the error of the ITs with the PMU, results in a term that is 200 times smaller than the addition of the errors. This makes the measurements performed by instrument transformers and by the PMUs to be independent and their contribution to the overall uncertainty to be additive. However, in the case that a more detailed measurement chain is considered, this independence of components in the measurement chain might not be valid. It should be noted though that the instrument transformers and the PMUs are the measurement chain components that introduce the largest error to the measurements.

From (12)-(15) it can be seen that if the error is treated as a random variable, then the total error introduced to the PMU measurements (from the two components) is the sum of two uniform distributions with different bounds. In this sense, the random variable that will represent the total error introduced from both components will follow a trapezoidal distribution [20] whose shape is shown in Fig. 3. It should be noted that the trapezoidal distribution is valid for all types of PMU measurements (magnitude and angle of voltage and current). Additionally, as it is shown from (12)-(15) the voltage and the current in the PMU measurements are assumed independent in this work and consequently their uncertainties will be uncorrelated. This assumption is valid since completely different voltage and current measurement channels are used in most of the industrial PMUs.

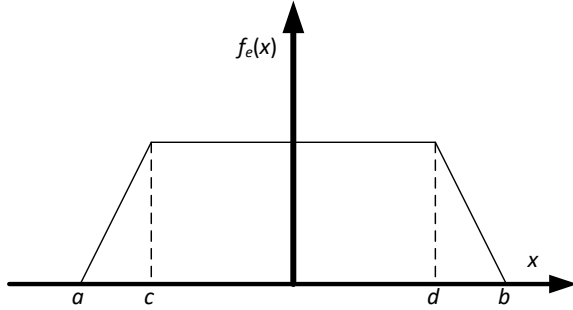


Fig. 3: Trapezoidal distribution of the PMU measurement chain error

According to [21], the variance of the trapezoidal distribution is calculated as,

$$\sigma^2 = \frac{a^2 + b^2 + c^2 + d^2 - ac - ad - bc - bd}{12}, \quad (16)$$

where,

$$a = -(\bar{e}_{IT} + \bar{e}_{PMU}) \quad (17)$$

$$b = (\bar{e}_{IT} + \bar{e}_{PMU}) \quad (18)$$

$$c = -(\bar{e}_{IT} - \bar{e}_{PMU}) \quad (19)$$

$$d = (\bar{e}_{IT} - \bar{e}_{PMU}) \quad (20)$$

Based on (17)-(20) the overall error introduced to the PMU measurements follows an isosceles trapezoidal distribution with known limits. Therefore, the calculation of the error variance will provide the overall uncertainty of each type of measurements provided by the PMU measurement chain. By substituting (17)-(20) into (16) the overall uncertainty of the PMU measurement chain for each type of measurements is,

$$u = \sqrt{\frac{\bar{e}_{IT}^2 + \bar{e}_{PMU}^2}{3}} \quad (21)$$

where  $\bar{e}_{IT}$  is the maximum error of the instrument transformer (either voltage or current transformer) for all the types of measurements, while  $\bar{e}_{PMU}$  is the maximum error of the PMU for all the types of measurements (magnitude and angle of voltage and current). It should be noted that (21) shows that the total squared uncertainty of the PMU measurements is the sum of the squared uncertainties of the two individual uniform distributions (PMUs and ITs), when no correlation between the instrument transformers and the PMUs is assumed.

Since the uncertainties of the measurements used for calculating the transmission line parameters can be obtained through (21), it is possible to approximate the uncertainties associated with the calculated line parameters according to the law of propagation of uncertainty [12]. Therefore, by assuming that the types of measurements provided by a PMU are uncorrelated, the combined standard uncertainty of the transmission line parameters can be calculated as,

$$u_p = \sqrt{\sum_{l=1}^8 \left[ \frac{\partial f_p(\mathbf{m})}{\partial \mathbf{m}(l)} u(\mathbf{m}(l)) \right]^2} \quad (22)$$

where,

$p$  represents the type of the line parameter ( $g_{sr}$ ,  $b_{sr}$ ,  $g_{sr}$ ) whose uncertainty is calculated

$f_p(\mathbf{m})$  is one of the equations (3)-(5) that are used for calculating the line parameters using PMU measurements

$$\mathbf{m} = [V_s \ V_r \ I_s \ I_r \ \phi_s \ \phi_r \ \theta_s \ \theta_r]$$

Through (22), the combined standard uncertainty of each line parameter can be calculated analytically. The partial derivatives for obtaining the analytic expressions of the uncertainties of each transmission line parameter are shown in the Appendix.

Since the uncertainty of the calculated line parameters is known, the expanded uncertainty can be calculated as [12],

$$U = ku \quad (23)$$

where  $k$  is the coverage factor which usually takes value between 2 and 3. In this sense, the calculated transmission line parameters can be associated with their confidence interval through the expanded uncertainty as,

$$p - U \leq P \leq p + U \quad (24)$$

where,

$P$  is the actual line parameter value and  $p$  is the calculated line parameter.

The proposed analytical calculation of the line parameter uncertainty considering both instrument transformer and PMU measurement errors results to a variable uncertainty that changes according to the operating condition of the power system. More specifically, as it is shown in (21), the uncertainty of the PMU measurements depends on the error of both the instrument transformer and the PMU, which essentially vary throughout the day. In the case of the PMU, both the voltage and current magnitude error are expressed as a percent of the measurand; hence, since the voltage and current vary throughout the day, the limits of the uniform distributions in (12) and (13) will vary as well. The same is true for the case of

the voltage transformer whose error is also expressed as a percent of the measurand. In the case of the current transformers, the maximum magnitude and angle errors of each accuracy class vary according to the loading of the current transformer. In particular, as it is shown in Table I in which the maximum magnitude error and phase displacement of several current transformers accuracy classes are depicted [22], the current magnitude and angle errors of each accuracy class vary according to the percentage of the rated current. Therefore, the proposed analytical expressions for calculating the uncertainty of the transmission line parameters consider the variability of the errors both due to the variations of the magnitude of the voltage and the current and the variable maximum error of the instrument transformer according to its loading condition.

The calculation procedure of the line parameters and the uncertainty bounds might be affected in case of bad PMU measurements (i.e., zero values). Therefore, a preprocessing of the measurement sample to identify and eliminate any bad measurements is recommended prior to the calculation of the line parameters and their associated uncertainty bounds [23].

TABLE I  
MAGNITUDE ERROR AND PHASE DISPLACEMENT - CURRENT TRANSFORMERS

Class	± Percentage of current error at percentage of rated current					± Phase displacement at percentage of rated current (degrees)				
	1	5	20	100	120	1	5	20	100	120
0.1	-	0.4	0.2	0.1	0.1	-	0.25	0.133	0.083	0.083
0.2S	0.75	0.35	0.2	0.2	0.2	0.5	0.25	0.167	0.167	0.167
0.2	-	0.75	0.35	0.2	0.2	-	0.5	0.25	0.167	0.167
0.5S	1.5	0.75	0.5	0.5	0.5	1.5	0.75	0.5	0.5	0.5
0.5	-	1.5	0.75	0.5	0.5	-	1.5	0.75	0.5	0.5
1	-	3	1.5	1	1	-	3	1.5	1	1

#### IV. EVALUATION OF THE EXPRESSIONS FOR THE UNCERTAINTIES OF LINE PARAMETERS

Without loss of generality, as an example, the analytical expressions that can be used for calculating the transmission line parameters uncertainty bounds are evaluated using the IEEE 14-bus system. The line parameters of the test system are calculated for a whole day through PMU measurements and consequently daily parameter bounds are obtained for a whole day. In order to have a more realistic representation of the real field conditions in the simulations, the actual line parameters are assumed to vary with the ambient temperature. In other words, the PMU measurements that are extracted for a whole day from the DigSilent software include the effect of line parameter variation due to temperature. In particular, the temperature varies between 24 °C to 39 °C following a daily pattern. The line parameters vary throughout the day with the ambient temperature as [13],

$$R(T) = R(T_o)[1 + \alpha(T - T_o)] \quad (25)$$

$$X(T) = X(T_o)[1 + \beta(T - T_o)] \quad (26)$$

where,

$T_o$  is the reference temperature, 20 °C;  $T$  is the ambient temperature;  $R(T)$ ,  $X(T)$  are the resistance and reactance of the line at temperature  $T$  respectively;  $R(T_o)$ ,  $X(T_o)$  is the resistance and reactance of the line at temperature  $T_o$  respectively;  $\alpha$ ,  $\beta$  are

the temperature coefficients of the resistance and reactance respectively and they are equal to 0.00393 (assuming an aluminium conductor) [24]. The uncertainties of the calculated line parameters are derived through (22) for the three parameters of each line and are used for defining the bounds of the parameters of each transmission line throughout the day. As indicated in (24) the bounds of each line parameter are obtained by using the expanded uncertainty of each parameter. In this work and without loss of generality the coverage factor that is used for the expanded uncertainty is chosen to be equal to 2.

#### A. PMU measurement generation

The IEEE-14 bus system is implemented in DigSilent software in which the daily load variation of Fig. 4 is assumed (total load of the system). The increase or decrease of the total load (Fig. 4) is attributed to each load of the system according to its contribution (percentage) to the total load in the system. The percentage of each load is calculated based on the values of the loads that are given in [25]. The PMU measurements are generated for a whole day by extracting the actual voltage and current phasor network values from DigSilent every 2 minutes and then random errors from a uniform distribution were introduced to the actual phasor values, reflecting the contribution to the measurement quality of the instrument transformers and the PMUs. In particular, two random errors were added in the magnitude and two random errors in the phase of the phasors (voltage and current). It should be noted that three different instrument transformers of accuracy classes 0.1, 0.2, and 0.5 are assumed, thus three different measurement sets (one for each IT class) are generated. The maximum errors of the three classes for the current transformers are shown in Table I, while the maximum errors for the voltage transformers are shown in Table II [26]. Moreover, the maximum errors of the PMUs are shown in Table III [27]. The maximum errors for the phase displacement of the PMU is obtained by assuming a Total Vector Error (TVE) equal to 1%. It should be noted that the maximum errors were used in the uniform distributions for generating the measurements obtained from a PMU measurement chain.

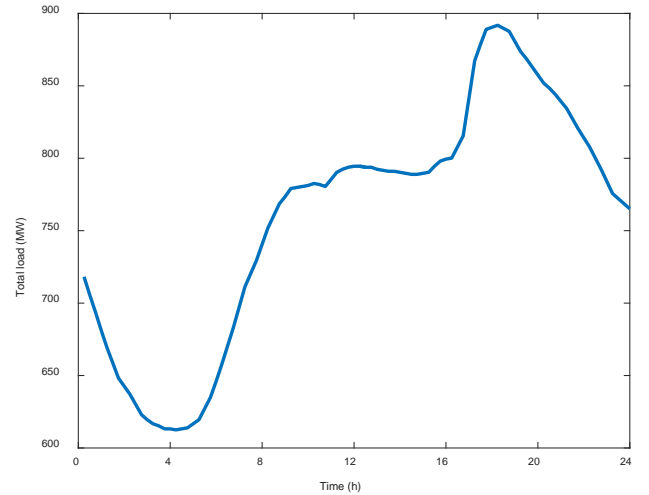


Fig. 4. Load variation for the IEEE 14-bus system

TABLE II  
MAGNITUDE ERROR AND PHASE DISPLACEMENT - VOLTAGE TRANSFORMERS

Accuracy class	± Percentage of voltage error	± Phase displacement (degrees)
0.1	0.1	0.083
0.2	0.2	0.167
0.5	0.5	0.333
1	1	0.667

TABLE III  
PMU MAXIMUM ERRORS

Voltage magnitude PMU (%)	Current magnitude PMU (%)	Phase angle PMU (degrees)
±0.02	±0.03	±0.54

As it is shown in Table I, the maximum error varies with the loading condition of the current transformer. Therefore, the maximum error of the uniform distribution associated with the current transformer errors changes throughout the day according to the loading conditions of the current transformers. For instance, the limit of the uniform distribution (of current magnitude) for a current transformer of 0.5 accuracy class in the interval 16:00-20:00 will be 0.5%, while in the interval 02:00-04:00 it will be 0.75%. The same is true for the phase error of the current transformers. It should be noted that the rated current of the current transformers is assumed to be 2 kA in the case studies.

#### B. An evaluation of the uncertainty bounds of the line parameters through Monte Carlo simulations

In order to evaluate whether the calculated line parameter bounds obtained by the calculated parameter uncertainties are representative for each line parameter, a Monte Carlo analysis is performed. In particular, a representative upper and lower bound for a parameter should enclose the line parameter that is calculated by the actual PMU measurements (containing any error that lies within the maximum and minimum error limits defined by the manufacturers). Therefore, each line parameter of the IEEE 14-bus system is calculated for 1000 times (Monte Carlo trials) for each accuracy class transformer. In each Monte Carlo trial random errors from the uniform distributions describing the measurement accuracy of the PMU and the ITs are introduced to the actual phasor values.

Ideally, the 1000 trials for each line parameter should be within the parameter's calculated lower and upper bounds that are obtained through (24). It should be noted that in each Monte Carlo trial the line parameters are calculated for the whole day, while the calculated bounds of the parameters for the whole day are obtained from one (the first) trial only. The number of Monte Carlo trials is determined as [28], [29],

$$N = (k\bar{s} / p)^2 \quad (27)$$

where  $\bar{s}$  is the standard deviation of the initial sample of Monte Carlo trials without using (27),  $k$  is the coverage factor (in this work  $k=2$ ), and  $p$  is the level of precision (in this work  $p=0.05$ ). The factor  $p$  is implicitly chosen such that the trials (calculated parameters) from the Monte Carlo simulation will have an absolute error of 0.05 from the mean of the  $N$  Monte Carlo trials. In this work, initially 100 Monte Carlo trials were executed, and the initial sample variance is calculated. It is worth mentioning that the Monte Carlo analysis is used only for

testing whether the calculated line parameters for 1000 times are within the derived parameter bounds. In other words, no Monte Carlo analysis is required for deriving the calculated bounds.

Since the line parameters are unlikely to change within short time intervals, the same bound is used for every one-hour interval of the day. In particular, the bounds (in the first Monte Carlo trial) are calculated every 2 minutes (as the line parameters) as shown in (24). The maximum upper bound from the one-hour time interval (out of the 30 upper bounds) is chosen as the representative upper bound for the one-hour time interval (right hand side of (24)), while the minimum value from the one-hour time interval (left hand side of (24)) is chosen as the representative lower bound of the one-hour time interval. The above procedure for determining the daily bounds of the line parameters is followed in the first Monte Carlo trial for all the one-hour time intervals of the day. As it is aforementioned, the coverage factor  $k$  is equal to 2 for the calculation of the expanded uncertainty. In Figs. 5, 6, and 7, the bounds of the susceptance of the line that connects buses 9 and 14 of the IEEE 14-bus system is shown in the cases that the susceptance is calculated when the PMU is connected to a 0.1, 0.2, and 0.5 accuracy class transformer. The 1000 calculations of the line susceptance (with solid line and different colors) as well as the actual susceptance values are also shown in the three figures. As it is indicated in the three figures, the reported values for the bounds and the calculated parameters are in p.u. The base value for the susceptance (Figs. 5-7) is  $5.74 \times 10^{-3}$  S; thus in order to find the actual value, the p.u values of the susceptance should be multiplied with the base value.

As it can be concluded from Figs. 5-7, the calculation of the expanded uncertainty for this line parameter through the proposed analytical expressions, considering both instrument transformer and PMU uncertainties, represents adequately the bounds of the calculated parameters. Furthermore, the calculated bounds of the susceptance differ according to the instrument transformer that is used in the PMU measurement chain. In particular, the bounds in the case of the 0.5 accuracy class transformer are larger than in the cases of 0.2 and 0.1 accuracy class transformers. This verifies that the analytical expression for the uncertainties of the calculated parameters can provide valid information regarding the accuracy of the calculated parameters according to the instrument transformers of the measurement chain. It is also worth mentioning that the bounds vary throughout the day indicating the best periods of the day that the line parameters can be calculated with less uncertainty. These periods are actually in line with the periods of the day with high loads, due to the smaller errors of the current transformers when they are fully loaded.

In Table IV, the number of times that the calculated parameters (i.e., series conductance and susceptance, and shunt susceptance) of all the lines of the IEEE 14-bus system are out of the calculated bounds in 1000 Monte Carlo trials are tabulated. It should be noted that the number of line parameters that should be calculated in the IEEE 14-bus system is 40 (excluding transformers). Each line parameter is calculated for one day for 1000 times and the time instants throughout the day that are out of its bounds are counted.



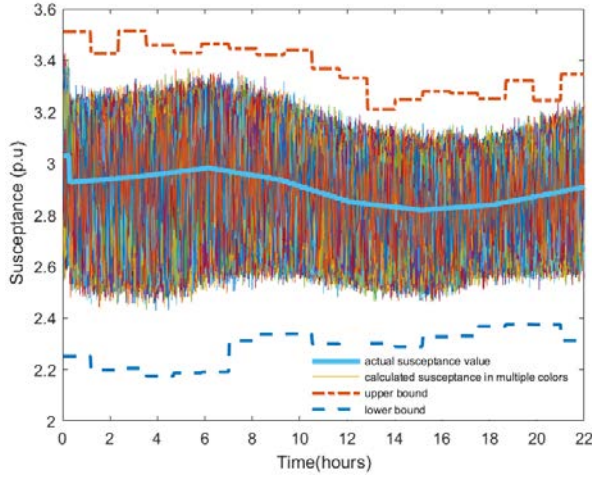


Fig. 5. Susceptance of line connecting buses 9 and 14 from a measurement chain with 0.1 instrument transformers

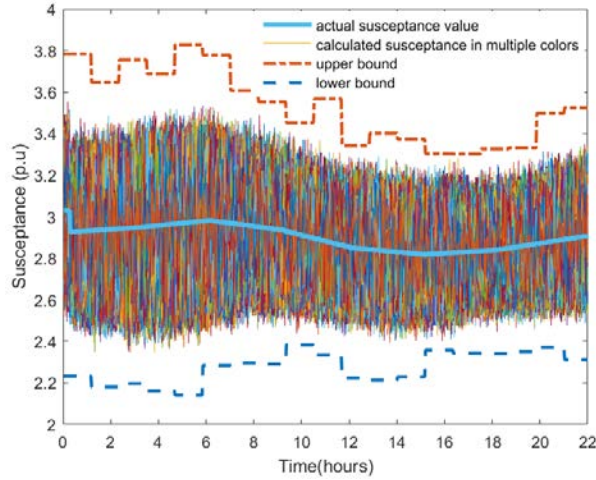


Fig. 6. Susceptance of line connecting buses 9 and 14 from a measurement chain with 0.2 instrument transformers

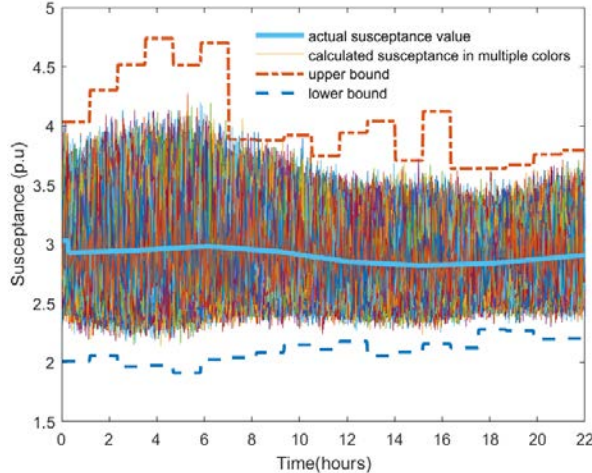


Fig. 7. Susceptance of line connecting buses 9 and 14 from a measurement chain with 0.5 instrument transformers

In the case of the 0.5 accuracy class transformer, in only 1230 time instants from  $28.8 \times 10^6$  time instants (40 parameters multiplied by 1000 Monte Carlo trials, multiplied by  $24 \times 60 / 2 = 720$  time instants of the day, where a 2-minute time granularity has been considered) the calculated parameters were

out of the calculated bounds. In other words, only 0.004% from all the line parameter calculations over one day, were not enclosed by the calculated bounds. The time instants that the line parameters were out of the bounds in the case of 0.2 accuracy class transformers were 266 (0.001% over all the line parameter calculations for one day), while in the case of 0.1 accuracy class transformers the time instants that the parameters were out of the calculated bounds were 79 (0.0003% over all the line parameter calculations). Through this analysis it can be concluded that the calculated bounds represent extremely accurately a large sample of the calculated line parameters throughout the day. This shows the validity of the calculated bounds since for only a negligible percentage of time instants the calculated parameters were out of bounds in 1000 Monte Carlo trials. Furthermore, in order to provide insights regarding the applicability of the uncertainty propagation law used in (22), the standard uncertainty that is calculated through (22) in one of the Monte Carlo trials (for a whole day) is compared to the standard deviation of the 1000 samples of the parameters (obtained through the Monte Carlo analysis). The average standard uncertainty difference in percent for each parameter (series conductance, series susceptance) is calculated for a whole day as,

$$\text{aver std difference (\%)} = \frac{1}{N} \sum_{l=1}^N \frac{|u_p^l - \bar{s}_p^l|}{\bar{s}_p^l} \times 100 \quad (28)$$

where,  $u_p^l$  is the standard uncertainty of each line parameter calculated through (22),  $\bar{s}_p^l$  is the standard deviation of each line parameter calculated from 1000 samples, and  $N$  is the number of time instants over one day that the parameters are calculated (in this work 720). Table V tabulates the mean value (over the number of lines in the system) of the standard deviation difference in percent for the series conductance and susceptance (for the three different accuracy classes). As it is shown in Table V, the standard uncertainty calculated through the uncertainty propagation law approximates the sample variance of the two types of parameters, since their percent difference is relatively small. In particular, this is more evident in the case of series susceptance where the largest percentage standard deviation difference is 2.5%. The percentage standard deviation difference of the conductance is larger than the one of the susceptance but still in acceptable limits to conclude that the uncertainty propagation law could be applied for the calculation of the uncertainty of the line parameters.

TABLE IV  
NUMBER OF TIME INSTANTS THAT PARAMETERS ARE OUTSIDE THE  
CALCULATED BOUNDS IN 1000 MONTE CARLO TRIALS

Instrument transformer accuracy class	Number of time instants that the parameters are outside the calculated bounds	Percentage of time instants outside the bounds (%)
0.5	1230	0.004
0.2	266	0.001
0.1	4	0.00001

TABLE V  
AVERAGE STANDARD UNCERTAINTY DIFFERENCE

Instrument transformer accuracy class	Series conductance ( $g_{sr}$ ) (%)	Series susceptance ( $b_{sr}$ ) (%)
0.1	28.3	2.5
0.2	24.9	1.7
0.5	19.8	2

### 1. Validation of the calculated bounds in case that the measurement errors do not follow a uniform distribution

In the real field, the distribution of the measurement errors is not known, while it is likely that their distribution is not uniform. In this case study, the calculated bounds are calculated by assuming that the measurement errors follow a uniform distribution as it is shown in Section III, however the PMU measurements are generated by introducing measurement errors from a quadratic U-distribution. The aim of this case study is to examine whether the calculated bounds enclose a large portion of the calculated line parameters from a Monte Carlo analysis (1000 trials) even if the error associated to the PMU measurements does not follow the assumed uniform distribution. The time instances that the calculated line parameters are out of the calculated bounds are also used as an evaluation metric. As it is shown in Table VI, the percentage of the time instants that the calculated line parameters lie outside the calculated bounds is increased for the three accuracy classes (comparing to Table IV), however it is still quite low. In particular, the percentage of time instants that are outside of the bounds in the case of the 0.5 accuracy class transformer is the larger one and equal to 0.035% (9850 over  $28 \times 10^6$  instants). This is because larger uncertainty is introduced to the measurement and consequently the uncertainty of the calculated line parameters is larger. However, the proposed analytical expressions still provide representative bounds for any of the three different accuracy class transformers, enclosing almost all the time instants where the line parameters are calculated (in 1000 trials), even if the measurement error distribution differs from the assumed one.

TABLE VI  
NUMBER OF TIME INSTANTS THAT PARAMETERS ARE OUTSIDE THE CALCULATED BOUNDS IN 1000 MONTE CARLO TRIALS (U DISTRIBUTION)

Instrument transformer accuracy class	Number of time instants that the parameters are outside the calculated bounds	Percentage of time instants outside the bounds (%)
0.5	9850	0.034
0.2	1238	0.004
0.1	660	0.002

### C. Importance of knowing the bounds of the calculated line parameters

The knowledge of the bounds of the calculated line parameters can be used for updating the settings of the distance relays that are used for the protection of the system in case of faults [14]. Furthermore, the bounds of the calculated parameters can be used for enhancing the situational awareness of the power system operators by using them in power system security analysis. In such analysis, the power system operators

check if the system will operate within the admissible limits in case of a contingency or increased power demand or transfer for one area to another. The P-V (Power-Voltage) curve is widely used for monitoring the voltage stability of the system in case of increased transfer of power from one area of the system to another. Actually, the P-V curve analysis comprises a series of power flow solutions for increasing power transfers and indicates the evolution of the voltages at the buses.

The transmission line parameters will play a critical role in the outcomes of the P-V analysis due to the dependence of the analysis on the power flow solutions. In particular, since the P-V analysis is a security analysis, it is important for the operators to know the worst scenarios that might lead the power system to instability. In such a case, it becomes useful to use the calculated upper and lower bounds of the transmission line parameters in order to monitor the evolvement of the system in the extreme cases that the calculated line parameters are in their bounds. This will provide valuable information to the power system operators regarding the stability of the system for increasing power transfers-for instance in the case of the peak loads.

In order to illustrate the importance of using the transmission line parameter bounds in the P-V analysis, the calculated bounds for the IEEE 14-bus system (shown in Fig. 8) as they are obtained for the Monte Carlo analysis of the previous section are used. In this sense, two case studies were performed. In the first case study, for extracting the P-V curves, the line parameters having the values of the upper bounds of the transmission line parameters of the system have been used; in the second case the values of the lower bounds have been used. For the P-V analysis in both cases, the generator of bus 2 that has a generation capability of 160 MW, was assumed that covers the load increase at buses 2, 3, 4, and 5 of the IEEE 14-bus system. The voltage magnitude resulting from the P-V analysis for bus 5 for the two case studies (upper and lower bounds) is shown in Fig. 9 for three different instrument transformer accuracy classes.

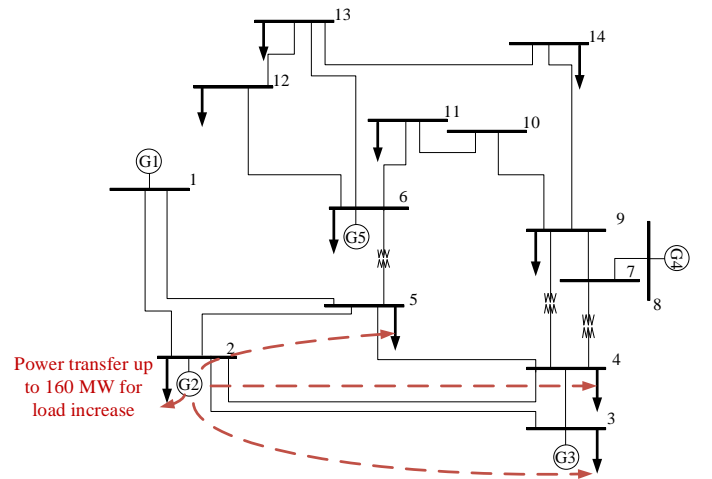


Fig. 8. Single line diagram of IEEE 14-bus system

As it is indicated in Fig. 9, the lower and upper bounds of the calculated line parameters can be used for defining the range of the voltage in the buses in case of power transfer. In this way, the power system operators can be aware of the upper and lower



limits of the voltage magnitude of the system given that the calculated line parameters used in the monitoring applications are characterized by an uncertainty. In other words, the study shows that in case that the generator of bus 2 needs to cover the load increase of loads 2, 3, 4, and 5 with its maximum generation output, the voltage limit of bus 5 is not violated (assuming voltage limits of 0.95 and 1.05 p.u.) even for the extreme line parameter bounds. Therefore, knowing the line parameter bounds, the operators can run such security analysis for ensuring the proper operation of the supervised network.

Since the P-V analysis relies on the power flow solution, there is a direct dependency on the line parameter values. This implies that if the actual line parameter values are between the uncertainty bounds that are calculated through the proposed methodology, the corresponding P-V curves will be translated into a family of curves bounded by the lower and upper limits that are shown in Fig. 9. In order to indicate such a case, for the same scenario as depicted in Fig. 9, the P-V curves of bus 4 for the lower and upper bounds of the line parameters (calculated for the 0.2 accuracy class instrument transformers), as well as the P-V curve extracted with the nominal parameter of the system, are shown in Fig. 10. As it is illustrated in Fig. 10, the P-V curve of the nominal line parameters lies between the P-V curves obtained from applying the upper and lower bounds of the line parameters. This indicates that using the upper and lower bounds of the line parameters in security analysis, the operators can have a visualization of the extreme values of the voltage magnitude of the buses. It is worth mentioning that this conclusion can be generalized for all the buses of the system.

Furthermore, through the P-V curves of the lower and upper bounds, the situational awareness of the system operator is enhanced considerably. For instance, in the case that generator 2 operates at 160 MW to serve loads 2, 3, 4, and 5, the PV curves of the bounds show that the voltage of bus 4 given the calculated line parameters from the PMU measurements (and 0.2 accuracy class instrument transformers) could be approximately between 0.97 and 1.01 p.u. This ensures that bus 4 will remain within the admissible limits (0.95-1.05) whatever the error in the calculated line parameter is, and at the same time keeps aware the operators that a further increase of the loads in that area could lead bus 4 to a voltage limit violation (given that the lower bound is closer to 0.95 p.u.

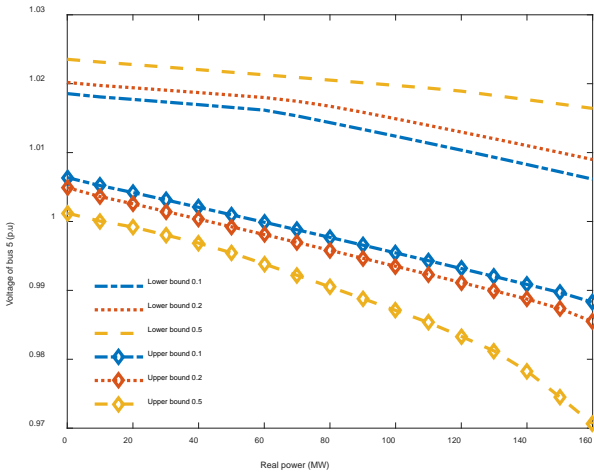


Fig. 9. P-V curve of bus 5

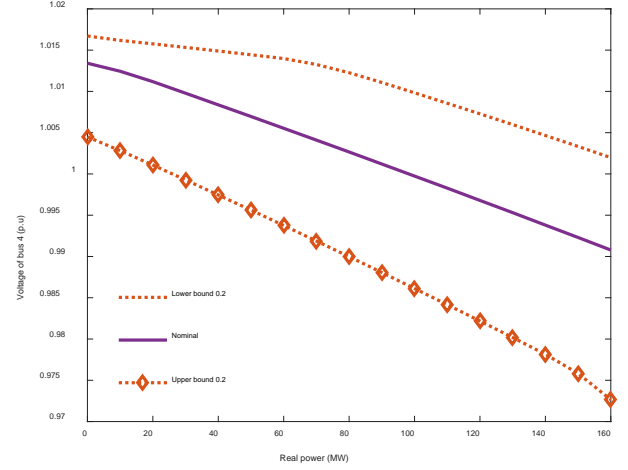


Fig. 10. P-V curves of bus 4

## V. CONCLUSIONS

In this paper the analytical calculation of the uncertainty of the line parameters estimated from PMU measurements is presented considering the random errors of a simplified measurement chain (both the instrument transformers and the PMU). The calculated combined uncertainties are used for defining the bounds of the line parameters when they are calculated from PMU measurements. These bounds can be used for enhancing the situational awareness of the power system operators when they perform security analysis. It is further shown through the Monte Carlo analysis that the calculated line parameter bounds encompass the calculated line parameters. This indicates the validity of the analytical expressions of the parameter uncertainty that are derived in this paper.

In practice, a measurement chain contains several other components either between the PMU and instrument transformer, or between the substation and the control center where the measurements are used (i.e., communication protocols, phasor data concentrators, communication links, etc). However, the latter will not impact the estimation of the line parameter since measurements are time tagged, while the same reporting rate of the PMUs is assumed in this work. Therefore, data aggregation procedures or communication delays will not impact the parameter calculation. The components in the measurement chain that could exist between the PMUs and the instrument transformers might introduce an additional uncertainty to the measurements, which is not considered in this work. It should be noted that for several components of the measurement chain, the quantification of their uncertainty is almost infeasible. For this work, the consideration of the additional uncertainty (from other components that were not considered in the measurement chain) can be achieved by increasing the coverage factor that is used for calculating the expanded uncertainty of the line parameters and consequently increasing the calculated parameter bounds interval.

## APPENDIX

According to (22) the uncertainties of the calculated line parameters can be derived by determining the partial

derivatives of the equations used for the calculation of the parameters over the PMU measurements. Following are the partial derivatives of (3)-(5) for calculating the combined uncertainties of the series conductance ( $g_{sr}$ ), the series susceptance ( $b_{sr}$ ), and the shunt susceptance ( $b_{sh}$ ).

The partial derivatives of the series conductance can be calculated as:

$$\frac{\partial g_{sr}}{\partial V_s} = \frac{D_{g_{sr}} \left[ 2AV_s \cos(c) + 3BV_s \cos(h) - I_r V_r^2 \cos(l) \right] - N_{g_{sr}} \left[ 4V_s^3 - 4V_s V_r^2 \cos(2\phi_s - 2\phi_r) \right]}{D_{g_{sr}}^2} \quad (29)$$

$$\frac{\partial g_{sr}}{\partial V_r} = \frac{D_{g_{sr}} \left[ I_s V_s^2 \cos(c) - 3AV_r \cos(d) - 2BV_r \cos(l) \right] - N_{g_{sr}} \left[ 4V_r^3 - 4V_s^2 V_r \cos(2\phi_s - 2\phi_r) \right]}{D_{g_{sr}}^2} \quad (30)$$

$$\frac{\partial g_{sr}}{\partial I_s} = \frac{V_r V_s^2 \cos(c) - V_r^3 \cos(d)}{D_{g_{sr}}} \quad (31)$$

$$\frac{\partial g_{sr}}{\partial I_r} = \frac{V_s^3 \cos(h) - V_s V_r^2 \cos(l)}{D_{g_{sr}}} \quad (32)$$

$$\frac{\partial g_{sr}}{\partial \phi_s} = \frac{D_{g_{sr}} \left[ 2AV_s^2 \sin(c) + B \left( V_s^2 \sin(h) - V_r^2 \sin(l) \right) \right] - 4N_{g_{sr}} V_s^2 V_r^2 \sin(2\phi_s - 2\phi_r)}{D_{g_{sr}}^2} \quad (33)$$

$$\frac{\partial g_{sr}}{\partial \phi_r} = \frac{D_{g_{sr}} \left[ A \left( -V_s^2 \sin(c) + V_r^2 \sin(d) \right) + 2BV_r^2 \sin(l) \right] + 4N_{g_{sr}} V_s^2 V_r^2 \sin(2\phi_s - 2\phi_r)}{D_{g_{sr}}^2} \quad (34)$$

$$\frac{\partial g_{sr}}{\partial \theta_s} = \frac{-AV_s^2 \sin(c) - AV_r^2 \sin(d)}{D_{g_{sr}}} \quad (35)$$

$$\frac{\partial g_{sr}}{\partial \theta_r} = \frac{-BV_s^2 \sin(h) - BV_r^2 \sin(l)}{D_{g_{sr}}} \quad (36)$$

where  $N_{g_{sr}}$ ,  $D_{g_{sr}}$  are the numerator and denominator of (3) that is used for calculating the series conductance.

The partial derivatives for the series susceptance can be calculated as:

$$\frac{\partial b_{sr}}{\partial V_s} = \frac{D_{b_{sr}} \left[ 2AV_s \sin(c) + 3BV_s \sin(h) + I_r V_r^2 \sin(l) \right] - N_{b_{sr}} \left[ 4V_s^3 - 4V_s V_r^2 \cos(2\phi_s - 2\phi_r) \right]}{D_{b_{sr}}^2} \quad (37)$$

$$\frac{\partial b_{sr}}{\partial V_r} = \frac{D_{b_{sr}} \left[ I_s V_s^2 \sin(c) + 3AV_r \sin(d) + 2BV_r \sin(l) \right] - N_{b_{sr}} \left[ 4V_r^3 - 4V_s^2 V_r \cos(2\phi_s - 2\phi_r) \right]}{D_{b_{sr}}^2} \quad (38)$$

$$\frac{\partial b_{sr}}{\partial I_s} = \frac{V_r V_s^2 \sin(c) + V_r^3 \sin(d)}{D_{b_{sr}}} \quad (39)$$

$$\frac{\partial b_{sr}}{\partial I_r} = \frac{V_s^3 \sin(h) + V_s V_r^2 \sin(l)}{D_{b_{sr}}} \quad (40)$$

$$D_{b_{sr}} \left[ -2AV_s^2 \cos(c) - B \left( V_s^2 \cos(h) + V_r^2 \cos(l) \right) \right] \quad (41)$$

$$\frac{\partial b_{sr}}{\partial \phi_s} = \frac{-4N_{b_{sr}} V_s^2 V_r^2 \sin(2\phi_s - 2\phi_r)}{D_{b_{sr}}^2}$$

$$\frac{\partial b_{sr}}{\partial V_s} = \frac{D_{b_{sr}} \left[ 2AV_s \sin(c) + 3BV_s \sin(h) + I_r V_r^2 \sin(l) \right] + N_{b_{sr}} \left[ 4V_s^3 - 4V_s V_r^2 \cos(2\phi_s - 2\phi_r) \right]}{D_{b_{sr}}^2} \quad (42)$$

$$\frac{\partial b_{sr}}{\partial \theta_s} = \frac{AV_s^2 \cos(c) - AV_r^2 \cos(d)}{D_{b_{sr}}} \quad (43)$$

$$\frac{\partial b_{sr}}{\partial \theta_r} = \frac{B \left( V_s^2 \cos(h) - V_r^2 \sin(l) \right)}{D_{b_{sr}}} \quad (44)$$

where,  $N_{b_{sr}}$ ,  $D_{b_{sr}}$  are the numerator and denominator of (4) that is used for calculating the series susceptance.

The partial derivatives of the shunt susceptance can be calculated as:

$$\frac{\partial b_{sh}}{\partial V_s} = \frac{D_{b_{sh}} \left[ I_s \sin(\theta_s - \phi_s) - I_r \sin(h) \right] - 2N_{b_{sh}} \left[ V_s - V_r \cos(\phi_s - \phi_r) \right]}{D_{b_{sh}}^2} \quad (45)$$

$$\frac{\partial b_{sh}}{\partial V_r} = \frac{D_{b_{sh}} \left[ -I_s \sin(d) + I_r \sin(\phi_r - \theta_r) \right] - 2N_{b_{sh}} \left[ V_r + V_s \cos(\phi_s - \phi_r) \right]}{D_{b_{sh}}^2} \quad (46)$$

$$\frac{\partial b_{sh}}{\partial I_s} = \frac{V_s \sin(\theta_s - \phi_s) - V_r \sin(d)}{D_{b_{sh}}} \quad (47)$$

$$\frac{\partial b_{sh}}{\partial I_r} = \frac{-V_s \sin(h) + V_r \sin(\phi_r - \theta_r)}{D_{b_{sh}}} \quad (48)$$

$$\frac{\partial b_{sh}}{\partial \phi_s} = \frac{D_{b_{sh}} \left[ -V_s I_s \cos(\theta_s - \phi_s) + B \cos(h) \right] - 2N_{b_{sh}} V_s V_r \sin(\phi_s - \phi_r)}{D_{b_{sh}}^2} \quad (49)$$

$$\frac{\partial b_{sh}}{\partial \phi_r} = \frac{D_{b_{sh}} \left[ -A \cos(d) + V_r I_r \cos(\phi_r - \theta_r) \right] - 2N_{b_{sh}} V_s V_r \sin(\phi_s - \phi_r)}{D_{b_{sh}}^2} \quad (50)$$

$$\frac{\partial b_{sh}}{\partial \theta_s} = \frac{V_s I_s \cos(\theta_s - \phi_s) + A \cos(d)}{D_{b_{sh}}} \quad (51)$$

$$\frac{\partial b_{sh}}{\partial \theta_r} = \frac{-B \cos(h) + V_r I_r \cos(\phi_r - \theta_r)}{D_{b_{sh}}} \quad (52)$$

where  $N_{b_{sh}}$ ,  $D_{b_{sh}}$  are the numerator and the denominator of (5) that is used for calculating the shunt susceptance.

## REFERENCES

- [1] M. Bockarjova and G. Andersson, "Transmission line conductor temperature impact on state estimator accuracy," in *IEEE PowerTech*, Lausanne, Jul. 2007.
- [2] Y. Wang and W. Xu, "Online tracking of transmission-line parameters using SCADA data," *IEEE Transactions on Power Delivery*, vol. 31, no. 2, pp. 674-682, Apr. 2016.
- [3] K. J. Kusic and D. L. Garrison, "Measurement of transmission line parameters from SCADA data," in *IEEE PES Power System Conference and Exposition*, New York, USA, Oct. 2004.
- [4] A. Abur and A. G. Exposito, *Power system state estimation: Theory and implementation*. New York: Basel, 2004.
- [5] M. Asprou and E. Kyriakides, "Identification and Estimation of erroneous transmission line parameters using PMU measurements," *IEEE Transactions on Power Delivery*, vol. 32, no. 6, pp. 2510-2519, Dec. 2017.
- [6] M. R. M. Castillo et al., "Offline detection, identification, and correction of branch parameter errors based on several measurement snapshots," *IEEE Transactions on Power Systems*, vol. 26, no. 2, pp. 870-877, May 2011.
- [7] S. Kurokawa, J. Pissolato, M. C. Tavares, C. M. Portela, and A. J. Prado, "A new procedure to derive transmission-line parameters: Applications and restrictions," *IEEE Transactions on Power Delivery*, vol. 21, no. 1, pp. 492-498, Jan. 2006.
- [8] L. Zhang and A. Abur, "Identifying parameter errors via multiple measurement scans," *IEEE Transactions on Power Systems*, vol. 28, no. 4, pp. 3916-3923, Nov. 2013.
- [9] RESERVE Project. [Online]. <http://www.re-serve.eu/>
- [10] R. E. Wilson, G. A. Zevenbergen, and D. L. Mah, "Calculation of transmission line parameters from synchronized measurements," *Electric Machines and Power Systems*, vol. 27, no. 12, pp. 1269-1278, 1999.
- [11] D. Shi, D. J. Tylavsky, K. M. Koellner, N. Logic, and D.E. Wheeler, "Transmission line parameter identification using PMU measurements," *European Transactions on Electrical Power*, vol. 21, no. 4, pp. 1574-1588, 2011.
- [12] "JGCM:Evaluation of the measurement data-Guide to the expression of uncertainty in measurements,JGCM100," 2008.
- [13] V. Cecchi, A. St. Leger, K. Miu, and O. C. Nwankpa, "Incorporating temperature variations into transmission line models," *IEEE Transactions on Power Delivery*, vol. 26, no. 4, pp. 2189-2196, Oct. 2011.
- [14] G. Sivanagaraju, S. Chakrabarti, and S. C. Srivastava, "Uncertainty in transmission line parameters: estimation and impact on line current differential protection," *IEEE Transactions on Instrumentation and Measurement*, vol. 63, no. 6, pp. 1496-1504, Jun. 2014.
- [15] D. Ritzmann, P. S. Wright, W. Holderbaum, and B. Potter, "A method for accurate transmission line impedance parameter estimation," *IEEE Transactions on Instrumentation and Measurement*, vol. 65, no. 10, pp. 2204-2213, Oct. 2016.
- [16] C. M. Roberts et al., "Improving distribution network model accuracy using impedance estimation from micro-synchrophasor data," in *2016 IEEE Power and Energy Society General Meeting*, Boston, MA, Jul. 2016, pp. 1-5.
- [17] M. Albu, E. Kyriakides, A.M. Dumitrescu, and I. M. Florea, "Analysis of distribution grids: State estimation using model uncertainties," in *2011 IEEE International Workshop on Applied Measurements for Power Systems (AMPS)*, Aachen, Germany, 2011, pp. 68-73.
- [18] P. A. Pegoraro, P. Castello, C. Muscas, K. Brady, and A. von Meier, "Handling Instrument Transformers and PMU Errors for the Estimation of Line Parameters in Distribution Grids," in *2017 IEEE International Workshop on Applied Measurements for Power Systems (AMPS)*, Liverpool, UK, Sep. 2017, pp. 1-6.
- [19] M. Asprou, E. Kyriakides, and M. Albu, "The effect of PMU measurement chain quality on line parameter calculation," in *IEEE International Instrumentation and Measurement Technology Conference (I2MTC)*, Turin, Italy, May 2017, pp. 1-6.
- [20] A. Mingotti, L. Peretto, R. Tinarelli, and K. Yiğit, "Simplified Approach to Evaluate the Combined Uncertainty in Measurement Instruments for Power Systems," *IEEE Transactions on Instrumentation and Measurement*, vol. 66, no. 9, pp. 2258-2265, Sep. 2017.
- [21] N. R. Kacker and J. F. Lawrence, "Trapezoidal and triangular distributions for Type B evaluation of standard uncertainty," *Metrologia*, vol. 44, no. 2, pp. 117-127, Feb. 2007.
- [22] "Instrument transformers-Part 2: Additional requirements for current transformers," IEC 61869-2:2012, 2012.
- [23] M. Asprou, E. Kyriakides, and M. Albu, "Bad data detection considering the accuracy of instrument transformers," in *2016 IEEE Power and Energy Society General Meeting (PESGM)*, Boston, MA, USA, Jul. 2016, pp. 1-5.
- [24] PowerFactory, Digsilent, 2016.
- [25] P. Demetriou, M. Asprou, J. Quiros-Tortos, and E. Kyriakides, "Dynamic IEEE Test Systems for Transient Analysis," *IEEE Systems Journal*, vol. 11, no. 4, pp. 2108-2117, Dec. 2017.
- [26] "Instrument transformers-Part 3: Additional requirements for inductive voltage transformers," IEC 61869-3:2011, 2011.
- [27] "Model 1133A GPS-Synchronized Power Quality/Revenue standard, Operation manual, Arbiter systems Inc.,CA, USA," Sep. 2006.
- [28] S.S. Agili, A. W. Morales, J. Li, and M. Resso, "Finding the Probability Distribution Functions of S-Parameters and Their Monte Carlo Simulation," *IEEE Transactions on Instrumentation and Measurement*, vol. 61, no. 11, pp. 2993-3002, Nov. 2012.
- [29] M. Liu, "Optimal number of trials for Monte Carlo simulation," Valuation Research Corporation, Article.